September 20-23, 2011
City of Cuernavaca México
XI International
Hydrogen Congress
an event of The Mexican Hydrogen Society
Cuernavaca...
The Endless Spring

ZEOLITES TYPE SBA-16 MODIFIED WITH PHOSPHOROUS AS PHOTOCATALYST FOR HYDROGEN PRODUCTION.

A. Pérez-Larios[a*], A Hernández-Gordillo[a], M. A. Guzman[b], R. Huirache-Acuña[c], R. Gómez[a]

[a]*Universidad Autónoma Metropolitana-Iztapalapa, Depto. de Química, Área de Catálisis, Grupo ECOCATAL, Av. San Rafael Atlixco No 189, México D.F., C.P. 09340, México.*

[b]*División Académica de Ciencias Biológicas, UJAT, Villahermosa, Tabasco, C. P. 8603, México*

[c]*Facultad de ingeniería Química, UMSNH, Morelia Michoacán, C.P. 58060, México.*

[*] contact email: mciqalex@gmail.com

ABSTRACT

In this work we studied zeolites type SBA-16, whit different percent of P (0, 0.5, 1.0, 1.5 and 2 %). The solids were characterized by; nitrogen adsorption (BET) and porosity (BJH), XRD patterns and UV-Vis spectroscopy. The photoactivity was evaluated using a Pyrex reactor of 200 ml using a solution ethanol-water (1:1 molar ratio) and 0.1 g of catalyst using a high pressure Hg lamp (with a wavelength of 254 nm and an intensity of 2.2 mW/cm^2 encapsulated in a quartz tube. The results showed materials with specific surface area among 942 to 755 m^2/g and mesopority characteristics. The XRD patterns show that a low angle is present the peak in 0.91° (110) is characteristic of cubic structure of this mesoporous material. The UV-Vis spectroscopy shown that regardless of the incorporation of phosphorus the catalysts have absorption at 500 nm. In the photodescomposition of ethanol:water, the evaluation has 800 μmol/h in the hydrogen.

Key words: SAB-16, phosphorous, hydrogen production, Ethanol.

1. INTRODUCTION

An important subject from the standpoint of both energy and environment is the production of clean hydrogen energy. Therefore the most ideal process for hydrogen production is to use solar energy for reduction of water to hydrogen[1]-[2]. In recent years, semiconductor oxide photocatalysis is gaining importance in the conversion of photon energy into chemical energy. Variety of photocatalysts mainly TiO_2 [3]-[4], MCM-41 [5] and Zeolitas-Y [6]-[10] oxides have been reported to be effective for the photocatalytic decomposition of water.

In another hand, mesoporous SBA-16 is a promising new semiconductor material as photocatalysts because of its large surface area (>800 m^2/g) and uniform hexagonal channels and a very narrow pore-size distribution considered as a type of zeolite [11]-[12]. Porous materials have attracted the interest of scientists and industry due to their potential applications, for instance in adsorption technology, molecular separation, gas sensors, etc. as well as photocatalysts due their electronic and optical properties. They are also known for their potential abilities to induce photocatalytic reactions [13]-[15].

The structure of SBA-16 can be described by a triply periodic minimal surface of I-WP (body centered, wrapped package). The mesophase might also be a triply periodic minimal surface. The open frameworks and tunable porosities endow SBA-16 mesoporous material with accessibility to metal ions and reagents such as a phosphate. These characteristics are extremely important in the fields of catalysis, sensors, electronic devices and nanotechnology [16].

In this work we studied zeolites type SBA-16 impregnated whit different percent of P(x) (x=0, 0.5, 1.0, 1.5 and 2.0 %). The solids were characterized by; (BET) and (BJH), XRD patterns and UV-Vis spectroscopy. To investigate the effect of the amount of the phosphorous on SBA-16 surface, the photocatalytic activity was evaluated in the hydrogen production reaction from ethanol-water decomposition.

2. EXPERIMENTAL

2.1. Support preparation

The mesoporous siliceous SBA-16 semiconductor was synthesized according the procedure described by Flodström and Alfredsson [17]. For the synthesis of SBA-16 material, Pluronic P127 ($EO_{106}PO_{70}EO_{106}$, BASF) was used as the structure directing agent. Typically, the Pluronic P127 was dissolved in a solution of water and HCl 2 M under stirring. After this, the required amount of tetraethyl orthosilicate (TEOS, 98%, Aldrich) was added to the solution, which was stirred at room temperature for 24 h. The mixture was subsequently transferred into polypropylene bottles and heated at 80 °C for 48 h. The solid was filtered, washed and dried at room temperature and then dried at 110 °C for 24 h. Finally, the sample was annealed at 550 °C in static air for 6 h. The mesoporous materials modification with phosphate was performed employing the post-synthesis method (grafting). Typically, the SBA-16 material was impregnated with aqueous solutions of H_3PO_4 of appropriate amount to obtain substrates with P_2O_5 loadings of 0.5, 1.0, 1.5, 2.0 wt%. After water evaporation at room temperature, the solid was dried at 110 °C for 4 h and then annealed at 500 °C for 4 h.

2.2. Characterization techniques

2.2.1. N_2 adsorption-desorption isotherms

The textural properties of the oxide semiconductor were determined from the adsorption-desorption isotherms of nitrogen at -196 °C, recorded with a Micromeritics TriStar 3000 apparatus. Prior to the experiments, the samples were degassed at 270 °C in vacuum for 5 h. The volume of the adsorbed N_2 was normalized to the standard temperature and pressure. The specific areas of the samples were calculated by applying the BET method to the nitrogen adsorption data within the 0.005-0.25 P/P_0 range. In order to avoid the tensile strength (TSE) artifact, the pore size distribution (PSD) curves were calculated by applying the Barret-Joyner-Halenda method (BJH) to the adsorption branches of the N_2 isotherms. The total pore volume (V_t) was obtained from the isotherms at $P/P_0 = 0.99$.

2.2.2. X-ray diffraction (XRD)

The semiconductor were characterized by powder X-ray diffractometry according to the step-scanning procedure (step size 0.02°; 0.5 s) with a computerized Seifert 3000 diffractometer, using Ni-filtered CuKα (λ = 0.15406 nm) radiation and a PW 2200 Bragg-Brentano *θ/2θ* goniometer equipped with a bent graphite monochromator and an automatic slit. The assignment of the various crystalline phases was based on the JPDS powder diffraction file cards.

2.2.3. DRS UV-Vis

The UV-vis diffuse reflectance spectra of the semiconductor were recorded in the range of 200-800 nm at room temperature using a Varian Cary 5000 UV-Vis spectrometer equipped with an integration sphere. The bandgap energy (Eg) was determined from absorption spectra using the Kubelka-Munk method.

2.2.4. Photocatalytic hydrogen production

The photocatalytic hydrogen production was performed in a Pyrex photoreactor system. It was filled with 200 ml of water-ethanol aqueous solution in a relation 1:1. The weight of semiconductor powder was 200 mg maintaining in suspension by magnetic stirring at room temperature to get the solution was not disturbing. The radiation energy was supplied by a high pressure of Hg lamp emitting λ=254 nm with I_0=4.4 mW/cm^2 encapsulated into a quartz tube which was immersed in the solution. The system was purged with N_2 for 30 min prior to eliminate the O_2 dissolved. The collect hydrogen gas was analyzed on Gas chromatograph using molecular sieve column, N_2 as a carrier gas and a thermal conductivity detector (TCD).

3. RESULTS AND DISCUSSION

3.1 Adsorption isotherms.

The N_2 adsorption-desorption isotherms for the SBA-16 semiconductor modified with different weigh percent of phosphorous (0, 0.5, 1, 1.5 y 2.0 wt %) are plotted in Figure 1. All the isotherms are of type IV according to IUPAC classification with a triangular hysteresis loop of type H-2 typical for materials with ink-bottle pores and pores network connectivity which is

characteristic of SBA-16 ([18]-[19]). Likewise, as phosphorous amount increases the specific surface area decrease but the pore diameter size was no modified that suggest no occlusion and/or obstruction of the porous was realized. It`s indicate that the phosphorous on surface was homogeneously impregnated (see Table 1) [20]-[21]. However, the semiconductor modified with 1.5 wt %, the specific surface area not show the decreasing linear, probably due to the incorporation of phosphorous on SBA-16 surface was no homogeneously carried out or the content is less than 1.0 wt %.

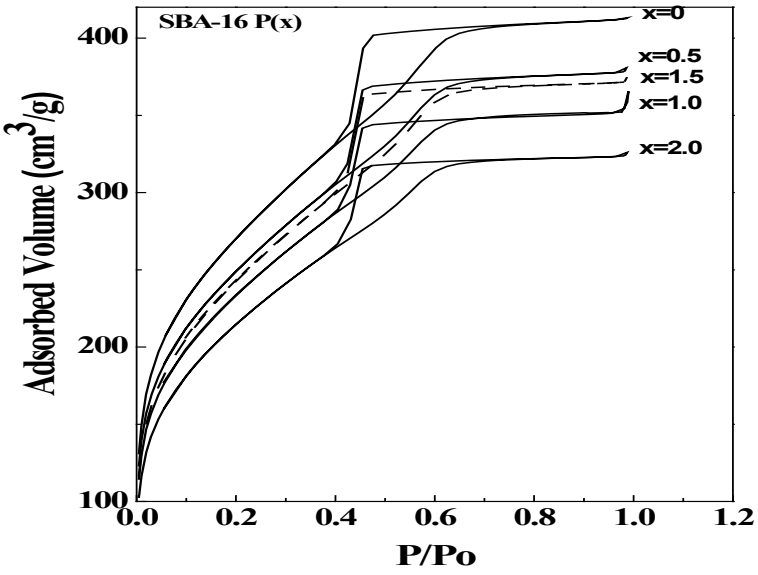

Figure 1 N_2 adsorption-desorption isotherms for SBA-16 P semiconductor synthesized at different amount of phosphorous (x).

Table 1 Textural properties of the SBA-16 materials.

Semiconductor (% of P)	S_g (m^2/g)	V_p (cm^3/g)	D_p *(nm)*
SBA-16	942	0.58	2.5
SBA-16 P (0.5)	868	0.54	2.5
SBA-16 P (1.0)	817	0.52	2.6
SBA-16 P (1.5)	852	0.54	2.5
SBA-16 P (2.0)	755	0.47	2.4

3.2 X-ray pattern

The X-ray patterns a low angle of the semiconductor annealed at 500 °C are presented in the Figure 2. We can observe than the samples present lightly changes in the intensity and amplitude of the peaks. The decreasing of the intensity of the peaks and narrow peaks can be related with the increment of the phosphorous content. In another hand, the samples one free of phosphorous present the highest cristallinity. The reflections of the XRD patterns of the SBA-16 pure (110), (200) y (211) could be indexed to the cubic body centered space group Im3m, thus providing an indication of the typical structures of SBA-16, patterns similar was finder by Klimova, and *et al.* [22], [23]and Amezcua, and *et al.* [24] on alumina and titanium modified SBA-16 support, respectively.

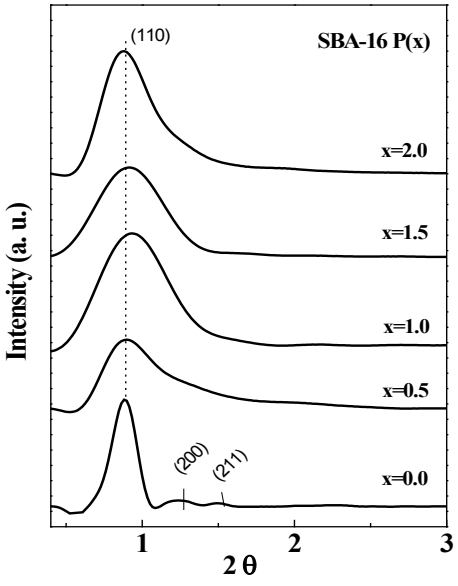

Figure 2 X-ray patterns for SBA-16 P semiconductor synthesized at different amount of phosphorous (x).

However, the position peaks of the reflections (110), (200) y (211) was displaced at 0.80°, 1.14°, y 1.39 ° en 2θ, respectively, when the phosphorous was deposited. This effect can be assigned to the relative change in the pore size to wall ratio and was also recently observed in the case of a mesoporous material by Kim *et al*.[25]. In our case, semiconductor with 0.5 and 1.5 wt % both present similar low intensity and broaden peaks, it suggests than the changes in the

pore size to wall ratio is similar probably due that the amount of phosphorous incorporated on SBA-16 surface is closed.

3.3 Diffuse reflectance spectroscopy UV-vis (DRS)

The optical properties for SBA-16 semiconductor were studied by diffuse reflectance spectroscopy UV-Vis. The absorption spectra UV-vis for the materials are shown in the Figure 3 as a function Kubelka-Munk-Schuster. All semiconductors show a change in the first wide absorption bands in the 450 to 400 nm region, due to the incorporation of the phosphorous on the SBA-16 surface. The second absorption bands in the 400 to 340 nm region were assigned to the absorption of the SBA-16 which the band gap value is close to 2.7 eV [26]. The optical properties suggest that these materials are capable to absorbed visible light to the conversion of photon energy into chemical energy which is necessary to hydrogen production. Taking the SAB-16 pure semiconductor as the blank, the absorption band in the 450 to 350 region rises as the amount of phosphorous was increased (into Figure 3). In this case, the absorption band of the SBA-16P semiconductor modified with 0.5 wt % of phosphorous was the lowest. In another hand, the semiconductor impregnated with 2.0 wt % of phosphorous exhibit absorption bands similar than the others one probably due to the phosphorous are highly disperse.

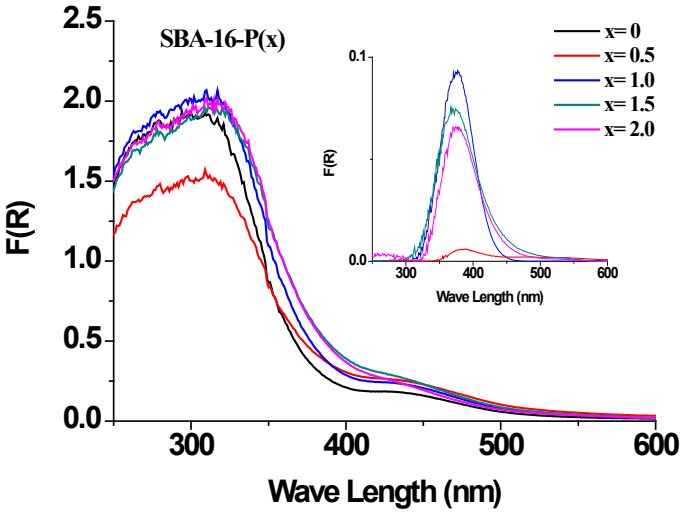

Figure 3 Diffuse reflectance absorption spectrum of phosphorous modified SBA-16.

3.4 Photocatalytic Activity in water splitting

The time course of hydrogen production reaction from ethanol-water decomposition is display in the Figure 4. We can observe than by increasing the content of phosphorous, the activity was improved to yield high hydrogen production (close to 2000 µmol/h). It´s indicate than the activity is related with the content of the phosphorous available. In another hand, these results indicate that the mesostructure is favorable for the interfacial separation of electron-hole pairs but also enable charge transport over longer distances. Likewise, we can observe that the samples modified with 1.0 and 1.5 wt % of phosphorous, presents the H_2 evolution rate higher (2000 µmol /h) than the other samples but the ended was diminished, presumably due to the deactivation as the time run. In the opposite, the samples modified with 2.0 wt % of phosphorous, the H_2 evolution rate was relatively low, however after the induction period, the H_2 evolution rate of 800 µmol/h was remained in the consecutive six hours and no deactivation was observed. The total production of H_2 reaches to 8000 µmol during the course of 10 h at appropriate amount of phosphorous.

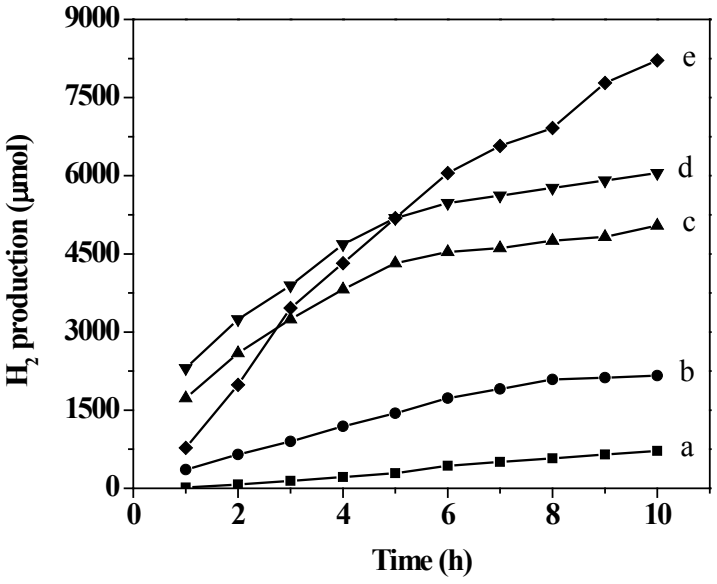

Figure 4 Hydrogen production profile for SBA-16 P (x) ; a=0, b=0.5, c=1.0, d=1.5 and e=2.0

4. CONCLUSION

The SBA-16 modified with different content of phosphorous synthesized by impregnation method exhibit properties interesting such as a high specific area, ordered of mesoporous where the phosphorous was homogeneously impregnated. Likewise these materials present absorption in the visible light region to convert the photon energy into chemical energy. Therefore, the optimal amount of phosphorous to obtain the maximum hydrogen production without deactivation is 2.0 wt % incorporated on SBA-16 surface homogeneously disperse. These results suggest that the phosphorous incorporated into another oxide metal surface is a good alternatively to produce hydrogen.

5. REFERENCES

[1] Fujishima, X. Zhang, D. A. Tryk, Int. J. Hydrogen Energy 32, 2664–2672 (2007).

[2] S. S. Rayalu, N. Dubey, N. K. Labhsetwar, S. Kagne, S. Devotta, Int. J. Hydrogen Energy 32, 2776–2783 (2007).

[3] J. S. Jang, S. J. Hong, J. Y. Kim, J. S. Lee, Chem. Phy. Lett. 475, 78–81 (2009).

[4] R. Sasikala, V. Sudarsan, C. Sudakar, R. Naik, T. Sakuntala, S. R. Bharadwaj, Int. J. Hydrogen Energy 33, 4966–4973 (2008).

[5] J. Alloys Comp. (2008).

[6] J. K. Reddy, G. Suresh, C.H. Hymavathi, V. D. Kumari, M. Subrahmanyam, Catal. Today 141, 89–93 (2009).

[7] S. Anandan, M. Yoon, J. Photochem. Photobiol. C: Photochem. Reviews 4, 5–18 (2003).

[8] R. Chatti, S. S. Rayalu, N. Dubey, N. Labhsetwar, S. Devotta, Solar Energy Mater. & Solar Cells 91, 180–190 (2007).

[9] R. V. Chatti, N. Dubey, M. V. Joshi, N. K. Labhsetwar, P.N. Joshi, S. S. Rayalu, Int. Hydrogen Energy 35, 1911–1920 (2010).

[10] N. Dubey, S. S. Rayalu, N. K. Labhsetwar, S. Devotta, Int. J. Hydrogen Energy 33, 5958-5966 (2008).

[11] G. Chao, Z. Dao and J. Guoxin, Chinese Science Bulletin 49, (3), 249-253 (2004).

[12] S-H Cho and S-E Park, From Zeolites to Porous MOF Materials – the 40th Anniversary of Int. Zeolite Confer. 641 (2007).

[13] E. M. Rivera-Muñoz and R. Huirache-Acuña, Int. J. Mol. Sci.; 11(9) 3069–3086 (2010).

[14] D. Zhao, J. Feng, Q. Huo, N. Melosh, GH Fredrickson, BF. Chmelka, GD Stucky, Science 279, 548–552 (1998)

[15] D. Zhao, Q. Huo, J. Feng, BF Chmelka, GD Stucky, J. Am. Chem. Soc., 120, 6024–6036 (1998).

[16] X. Chen, Y-S Jun, K. Takanabe, K. Maeda, K. Domen, X. Fu, M. Antonietti, and X. Wang, Chem. Mater., 21, 4093–4095 (2009).

[17] K. Flodström, V. Alfredsson, Micropor. Mesopor. Mater., 59, 167 (2003).

[18] K. S. W. Sing, D. H. Everett, R. A. W. Haul, L. Moscou, R. A. Pierotti, J. Rouquerol, and T. Siemieniewska, Pure and Applied Chemistry, 57 (4), 603–619 (1985).

[19] T. Gutiérrez, M. Romero, C. Leocadio, Z. Fuentes and T. Klimova, Revista del AMIDIQ 179-187 (2006).

[20] G. Leofantia, M. Padovanb, G. Tozzolac, B. Venturelli, Catal. Today 41, 207-219 (1998).

[21] J.C. Groen, L.A.A. Peffer, J. Pérez-Ramírez, Microp. Mesop. Mat. 60, 1–17 (2003).

[22] T. Klimova and L. Appl. Catal. B: Enviromental 139-150 (2008).

[23] T. Klimova, L. Lizama, L. Amezcua, P. Roquero, E. Terrés, J. Navarrete and J. Domínguez, Catal. Today 141-150 (2004).

[24] J. Amezcua, L. Lizama, C. Salcedo, I. Puente, J.M. Domínguez and T. Klimova, Catal. Today 578-588 (2005).

[25] T. W. Kim, F. Kleitz, B. Paul, and R. Ryoo. J. Am. Chem. Soc., 127 (20), 7601–7610 (2005).

[26] J.G. Graselli, B.J. Bulkin, Analytical Raman Spectroscopy, Wiley, New York, 352 (1991).